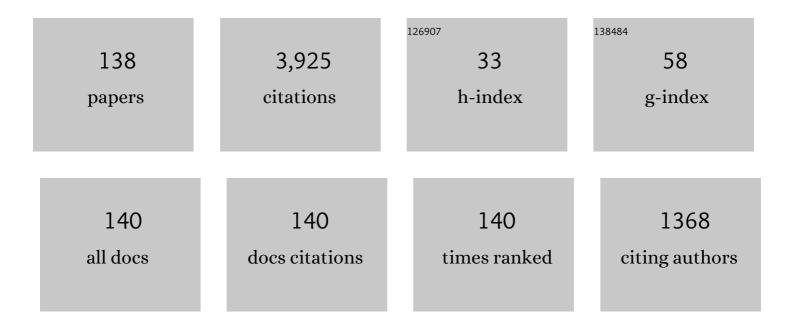
List of Publications by Year in descending order

Source: https://exaly.com/author-pdf/48290/publications.pdf Version: 2024-02-01



FUNC IF WOO

#	Article	IF	CITATIONS
1	Magnetic resonance electrical impedance tomography (MREIT): simulation study of J-substitution algorithm. IEEE Transactions on Biomedical Engineering, 2002, 49, 160-167.	4.2	251
2	Magnetic resonance electrical impedance tomography (MREIT) for high-resolution conductivity imaging. Physiological Measurement, 2008, 29, R1-R26.	2.1	191
3	Conductivity and current density image reconstruction using harmonicBzalgorithm in magnetic resonance electrical impedance tomography. Physics in Medicine and Biology, 2003, 48, 3101-3116.	3.0	178
4	Reconstruction of conductivity and current density images using only one component of magnetic field measurements. IEEE Transactions on Biomedical Engineering, 2003, 50, 1121-1124.	4.2	177
5	Magnetic Resonance Electrical Impedance Tomography (MREIT). SIAM Review, 2011, 53, 40-68.	9.5	136
6	J-substitution algorithm in magnetic resonance electrical impedance tomography (MREIT): phantom experiments for static resistivity images. IEEE Transactions on Medical Imaging, 2002, 21, 695-702.	8.9	108
7	Multi-Frequency Electrical Impedance Tomography System With Automatic Self-Calibration for Long-Term Monitoring. IEEE Transactions on Biomedical Circuits and Systems, 2014, 8, 119-128.	4.0	101
8	Noise analysis in magnetic resonance electrical impedance tomography at 3 and 11 T field strengths. Physiological Measurement, 2005, 26, 875-884.	2.1	92
9	Electrical conductivity images of biological tissue phantoms in MREIT. Physiological Measurement, 2005, 26, S279-S288.	2.1	91
10	Three-dimensional forward solver and its performance analysis for magnetic resonance electrical impedance tomography (MREIT) using recessed electrodes. Physics in Medicine and Biology, 2003, 48, 1971-1986.	3.0	87
11	Multi-frequency EIT system with radially symmetric architecture: KHU Mark1. Physiological Measurement, 2007, 28, S183-S196.	2.1	86
12	A fully parallel multi-frequency EIT system with flexible electrode configuration: KHU Mark2. Physiological Measurement, 2011, 32, 835-849.	2.1	86
13	<i>In Vivo</i> High-ResolutionConductivity Imaging of the Human Leg Using MREIT: The First Human Experiment. IEEE Transactions on Medical Imaging, 2009, 28, 1681-1687.	8.9	84
14	Image reconstruction of anisotropic conductivity tensor distribution in MREIT: computer simulation study. Physics in Medicine and Biology, 2004, 49, 4371-4382.	3.0	83
15	Validation of a multi-frequency electrical impedance tomography (mfEIT) system KHU Mark1: impedance spectroscopy and time-difference imaging. Physiological Measurement, 2008, 29, 295-307.	2.1	83
16	Error Analysis of Nonconstant Admittivity for MR-Based Electric Property Imaging. IEEE Transactions on Medical Imaging, 2012, 31, 430-437.	8.9	83
17	Electrical Conductivity Imaging Using Gradient <tex>\$B_z\$</tex> Decomposition Algorithm in Magnetic Resonance Electrical Impedance Tomography (MREIT). IEEE Transactions on Medical Imaging, 2004, 23, 388-394.	8.9	82
18	Finite element analyses of uniform current density electrodes for radio-frequency cardiac ablation. IEEE Transactions on Biomedical Engineering, 2000, 47, 32-40.	4.2	77

#	Article	IF	CITATIONS
19	<i>In vivo</i> electrical conductivity imaging of a canine brain using a 3 T MREIT system. Physiological Measurement, 2008, 29, 1145-1155.	2.1	74
20	Static conductivity imaging using variational gradientBzalgorithm in magnetic resonance electrical impedance tomography. Physiological Measurement, 2004, 25, 257-269.	2.1	70
21	Measurement of induced magnetic flux density using injection current nonlinear encoding (ICNE) in MREIT. Physiological Measurement, 2007, 28, 117-127.	2.1	61
22	Electrical Tissue Property Imaging at Low Frequency Using MREIT. IEEE Transactions on Biomedical Engineering, 2014, 61, 1390-1399.	4.2	55
23	Uniqueness and convergence of conductivity image reconstruction in magnetic resonance electrical impedance tomography. Inverse Problems, 2003, 19, 1213-1225.	2.0	50
24	Calibration methods for a multi-channel multi-frequency EIT system. Physiological Measurement, 2007, 28, 1175-1188.	2.1	49
25	Dependence of apparent resistance of four-electrode probes on insertion depth. IEEE Transactions on Biomedical Engineering, 2000, 47, 41-48.	4.2	47
26	Static resistivity image of a cubic saline phantom in magnetic resonance electrical impedance tomography (MREIT). Physiological Measurement, 2003, 24, 579-589.	2.1	47
27	Harmonic Decomposition in PDE-Based Denoising Technique for Magnetic Resonance Electrical Impedance Tomography. IEEE Transactions on Biomedical Engineering, 2005, 52, 1912-1920.	4.2	42
28	A Fidelity-Embedded Regularization Method for Robust Electrical Impedance Tomography. IEEE Transactions on Medical Imaging, 2018, 37, 1970-1977.	8.9	42
29	Ex Vivo and In Silico Feasibility Study of Monitoring Electric Field Distribution in Tissue during Electroporation Based Treatments. PLoS ONE, 2012, 7, e45737.	2.5	40
30	Reconstruction of current density distributions in axially symmetric cylindrical sections using one component of magnetic flux density: computer simulation study. Physiological Measurement, 2003, 24, 565-577.	2.1	39
31	Conductivity imaging of canine brain using a 3 T MREIT system: postmortem experiments. Physiological Measurement, 2007, 28, 1341-1353.	2.1	38
32	Anisotropic Conductivity Tensor Imaging of <italic>In Vivo</italic> Canine Brain Using DT-MREIT. IEEE Transactions on Medical Imaging, 2017, 36, 124-131.	8.9	37
33	MREIT conductivity imaging of the postmortem canine abdomen using CoReHA. Physiological Measurement, 2009, 30, 957-966.	2.1	36
34	Anisotropic conductivity tensor imaging in MREIT using directional diffusion rate of water molecules. Physics in Medicine and Biology, 2014, 59, 2955-2974.	3.0	36
35	Current Density Imaging During Transcranial Direct Current Stimulation Using DT-MRI and MREIT: Algorithm Development and Numerical Simulations. IEEE Transactions on Biomedical Engineering, 2016, 63, 168-175.	4.2	33
36	Conductivity image reconstruction from defective data in MREIT: numerical Simulation and animal experiment. IEEE Transactions on Medical Imaging, 2006, 25, 168-176.	8.9	31

#	Article	IF	CITATIONS
37	Performance evaluation of wideband bio-impedance spectroscopy using constant voltage source and constant current source. Measurement Science and Technology, 2012, 23, 105703.	2.6	31
38	Evaluation of Hepatoprotective Effect of Curcumin on Liver Cirrhosis Using a Combination of Biochemical Analysis and Magnetic Resonance-Based Electrical Conductivity Imaging. Mediators of Inflammation, 2018, 2018, 1-9.	3.0	29
39	Experimental performance evaluation of multiâ€echo ICNE pulse sequence in magnetic resonance electrical impedance tomography. Magnetic Resonance in Medicine, 2011, 66, 957-965.	3.0	28
40	Electrical Impedance Spectroscopy for Electro-Mechanical Characterization of Conductive Fabrics. Sensors, 2014, 14, 9738-9754.	3.8	28
41	Electrical tissue property imaging using MRI at dc and Larmor frequency. Inverse Problems, 2012, 28, 084002.	2.0	26
42	Electrodeless conductivity tensor imaging (CTI) using MRI: basic theory and animal experiments. Biomedical Engineering Letters, 2018, 8, 273-282.	4.1	25
43	Conductivity Tensor Imaging of <i>In Vivo</i> Human Brain and Experimental Validation Using Giant Vesicle Suspension. IEEE Transactions on Medical Imaging, 2019, 38, 1569-1577.	8.9	25
44	Multi-frequency time-difference complex conductivity imaging of canine and human lungs using the KHU Mark1 EIT system. Physiological Measurement, 2009, 30, S149-S164.	2.1	24
45	High field MREIT: setup and tissue phantom imaging at 11 T. Physiological Measurement, 2006, 27, S261-S270.	2.1	23
46	Regional absolute conductivity reconstruction using projected current density in MREIT. Physics in Medicine and Biology, 2012, 57, 5841-5859.	3.0	23
47	Feasibility of magnetic resonance electrical impedance tomography (MREIT) conductivity imaging to evaluate brain abscess lesion: <i>In vivo</i> canine model. Journal of Magnetic Resonance Imaging, 2013, 38, 189-197.	3.4	23
48	Temperature measurement within myocardium during in vitro RF catheter ablation. IEEE Transactions on Biomedical Engineering, 2000, 47, 1518-1524.	4.2	22
49	Ramp-Preserving Denoising for Conductivity Image Reconstruction in Magnetic Resonance Electrical Impedance Tomography. IEEE Transactions on Biomedical Engineering, 2011, 58, 2038-2050.	4.2	21
50	lon mobility imaging and contrast mechanism of apparent conductivity in MREIT. Physics in Medicine and Biology, 2011, 56, 2265-2277.	3.0	21
51	Software Toolbox for Low-Frequency Conductivity and Current Density Imaging Using MRI. IEEE Transactions on Biomedical Engineering, 2017, 64, 2505-2514.	4.2	20
52	Portable multi-parameter electrical impedance tomography for sleep apnea and hypoventilation monitoring: feasibility study. Physiological Measurement, 2018, 39, 124004.	2.1	20
53	Electrical conductivity imaging using a variational method in B z -based MREIT. Inverse Problems, 2005, 21, 969-980.	2.0	18
54	Integrated EIT system for functional lung ventilation imaging. BioMedical Engineering OnLine, 2019, 18, 83.	2.7	18

#	Article	IF	CITATIONS
55	Mathematical framework for Bz-based MREIT model in electrical impedance imaging. Computers and Mathematics With Applications, 2006, 51, 817-828.	2.7	17
56	Integration of the denoising, inpainting and local harmonic <i>B_z</i> algorithm for MREIT imaging of intact animals. Physics in Medicine and Biology, 2010, 55, 7541-7556.	3.0	17
57	Simultaneous imaging of dualâ€frequency electrical conductivity using a combination of <scp>MREIT</scp> and <scp>MREPT</scp> . Magnetic Resonance in Medicine, 2014, 71, 200-208.	3.0	17
58	Identification of current density distribution in electrically conducting subject with anisotropic conductivity distribution. Physics in Medicine and Biology, 2005, 50, 3183-3196.	3.0	16
59	Optimization of current injection pulse width in MREIT. Physiological Measurement, 2007, 28, N1-N7.	2.1	16
60	A tissue-relaxation-dependent neighboring method for robust mapping of the myelin water fraction. Neurolmage, 2013, 74, 12-21.	4.2	16
61	Non-iterative harmonic <i> B _z </i> algorithm in MREIT. Inverse Problems, 2011, 27, 085003.	2.0	15
62	Simulations and phantom evaluations of magnetic resonance electrical impedance tomography (MREIT) for breast cancer detection. Journal of Magnetic Resonance, 2013, 230, 40-49.	2.1	15
63	Multilayered Fabric Pressure Sensor for Real-Time Piezo-Impedance Imaging of Pressure Distribution. IEEE Transactions on Instrumentation and Measurement, 2020, 69, 565-572.	4.7	15
64	Three-dimensional MREIT simulator of static bioelectromagnetism and MRI. Biomedical Engineering Letters, 2011, 1, 129-136.	4.1	14
65	Fast conductivity imaging in magnetic resonance electrical impedance tomography (MREIT) for RF ablation monitoring. International Journal of Hyperthermia, 2014, 30, 447-455.	2.5	13
66	Reconstruction of dual-frequency conductivity by optimization of phase map in MREIT and MREPT. BioMedical Engineering OnLine, 2014, 13, 24.	2.7	13
67	Magnetic flux density measurement in magnetic resonance electrical impedance tomography using a low-noise current source. Measurement Science and Technology, 2011, 22, 105803.	2.6	13
68	Direct detection of neural activity in vitro using magnetic resonance electrical impedance tomography (MREIT). NeuroImage, 2017, 161, 104-119.	4.2	12
69	Extracellular Total Electrolyte Concentration Imaging for Electrical Brain Stimulation (EBS). Scientific Reports, 2018, 8, 290.	3.3	12
70	Low-frequency dominant electrical conductivity imaging of in vivo human brain using high-frequency conductivity at Larmor-frequency and spherical mean diffusivity without external injection current. Neurolmage, 2021, 225, 117466.	4.2	12
71	Feature Extraction of Upper Airway Dynamics during Sleep Apnea using Electrical Impedance Tomography. Scientific Reports, 2020, 10, 1637.	3.3	12
72	Basic setup for breast conductivity imaging using magnetic resonance electrical impedance tomography. Physics in Medicine and Biology, 2006, 51, 443-455.	3.0	11

#	Article	IF	CITATIONS
73	<i>In Vivo</i> Measurement of Brain Tissue Response After Irradiation: Comparison of T2 Relaxation, Apparent Diffusion Coefficient, and Electrical Conductivity. IEEE Transactions on Medical Imaging, 2019, 38, 2779-2784.	8.9	11
74	Noninvasive, simultaneous, and continuous measurements of stroke volume and tidal volume using EIT: feasibility study of animal experiments. Scientific Reports, 2020, 10, 11242.	3.3	11
75	Validation of conductivity tensor imaging using giant vesicle suspensions with different ion mobilities. BioMedical Engineering OnLine, 2020, 19, 35.	2.7	11
76	Highâ€frequency electrical properties tomography at 9.4T as a novel contrast mechanism for brain tumors. Magnetic Resonance in Medicine, 2021, 86, 382-392.	3.0	11
77	Radiofrequency ablation lesion detection using MR-based electrical conductivity imaging: A feasibility study of <i>ex vivo</i> liver experiments. International Journal of Hyperthermia, 2013, 29, 643-652.	2.5	10
78	Numerical Simulations of MREIT Conductivity Imaging for Brain Tumor Detection. Computational and Mathematical Methods in Medicine, 2013, 2013, 1-10.	1.3	10
79	Alternating steady state free precession for estimation of current-induced magnetic flux density: A feasibility study. Magnetic Resonance in Medicine, 2016, 75, 2009-2019.	3.0	10
80	Precision constant current source for electrical impedance tomography. , 0, , .		9
81	Reconstruction of conductivity using the dual-loop method with one injection current in MREIT. Physics in Medicine and Biology, 2010, 55, 7523-7539.	3.0	9
82	Analysis of local projected current density from one component of magnetic flux density in MREIT. Inverse Problems, 2013, 29, 075001.	2.0	9
83	In vivo mapping of current density distribution in brain tissues during deep brain stimulation (DBS). AIP Advances, 2017, 7, 015004.	1.3	9
84	Mathematical framework for a new microscopic electrical impedance tomography system. Inverse Problems, 2011, 27, 055008.	2.0	8
85	Improved conductivity image of human lower extremity using MREIT with chemical shift artifact correction. Biomedical Engineering Letters, 2012, 2, 62-68.	4.1	8
86	Detection of temperature distribution via recovering electrical conductivity in MREIT. Physics in Medicine and Biology, 2013, 58, 2697-2711.	3.0	8
87	Optimal geometry toward uniform current density electrodes. Inverse Problems, 2011, 27, 075004.	2.0	7
88	Noise analysis in fast magnetic resonance electrical impedance tomography (MREIT) based on spoiled multi gradient echo (SPMGE) pulse sequence. Physics in Medicine and Biology, 2014, 59, 4723-4738.	3.0	7
89	Experimental evaluation of electrical conductivity imaging of anisotropic brain tissues using a combination of diffusion tensor imaging and magnetic resonance electrical impedance tomography. AIP Advances, 2016, 6, .	1.3	7
90	A Pathophysiological Validation of Collagenase II-Induced Biochemical Osteoarthritis Animal Model in Rabbit. Tissue Engineering and Regenerative Medicine, 2018, 15, 437-444.	3.7	7

#	Article	IF	CITATIONS
91	Extracellular electrical conductivity property imaging by decomposition of high-frequency conductivity at Larmor-frequency using multi-b-value diffusion-weighted imaging. PLoS ONE, 2020, 15, e0230903.	2.5	7
92	Phase artefact reduction in magnetic resonance electrical impedance tomography (MREIT). Physics in Medicine and Biology, 2006, 51, 5277-5288.	3.0	6
93	Experimental validations of in vivo human musculoskeletal tissue conductivity images using MRâ€based electrical impedance tomography. Bioelectromagnetics, 2014, 35, 363-372.	1.6	6
94	Sub-millimeter resolution electrical conductivity images of brain tissues using magnetic resonance-based electrical impedance tomography. Applied Physics Letters, 2015, 107, .	3.3	6
95	A method for MREIT-based source imaging: simulation studies. Physics in Medicine and Biology, 2016, 61, 5706-5723.	3.0	6
96	Real-Time Identification of Upper Airway Occlusion Using Electrical Impedance Tomography. Journal of Clinical Sleep Medicine, 2019, 15, 563-571.	2.6	6
97	Source Consistency Electrical Impedance Tomography. SIAM Journal on Applied Mathematics, 2020, 80, 499-520.	1.8	6
98	MRâ€Based Electrical Conductivity Imaging of Liver Fibrosis in an Experimental Rat Model. Journal of Magnetic Resonance Imaging, 2021, 53, 554-563.	3.4	6
99	EIT Imaging of Upper Airway to Estimate Its Size and Shape Changes During Obstructive Sleep Apnea. Annals of Biomedical Engineering, 2019, 47, 990-999.	2.5	5
100	Digital phase-sensitive demodulator for electrical impedance tomography. , 0, , .		4
101	In vivo magnetic resonance electrical impedance tomography of canine brain: Disease model study of ischemia and abscess. Biomedical Engineering Letters, 2011, 1, 56-61.	4.1	4
102	Improved conductivity reconstruction from multi-echo MREIT utilizing weighted voxel-specific signal-to-noise ratios. Physics in Medicine and Biology, 2012, 57, 3643-3659.	3.0	4
103	Optimization of magnetic flux density for fast MREIT conductivity imaging using multi-echo interleaved partial fourier acquisitions. BioMedical Engineering OnLine, 2013, 12, 82.	2.7	4
104	Optimization of magnetic flux density measurement using multiple RF receiver coils and multi-echo in MREIT. Physics in Medicine and Biology, 2014, 59, 4827-4844.	3.0	4
105	Reconstruction of apparent orthotropic conductivity tensor image using magnetic resonance electrical impedance tomography. Journal of Applied Physics, 2015, 117, 104701.	2.5	4
106	A harmonic -based conductivity reconstruction method in MREIT with influence of non-transversal current density. Inverse Problems in Science and Engineering, 2018, 26, 811-833.	1.2	4
107	Anisotropic conductivity tensor imaging for transcranial direct current stimulation (tDCS) using magnetic resonance diffusion tensor imaging (MR-DTI). PLoS ONE, 2018, 13, e0197063.	2.5	4
108	Noninvasive Beat-To-Beat Stroke Volume Measurements to Determine Preload Responsiveness During Mini-Fluid Challenge in a Swine Model: A Preliminary Study. Shock, 2021, 56, 850-856.	2.1	4

#	Article	IF	CITATIONS
109	Influence of current injection scheme on electrical impedance tomography for monitoring of the respiratory function of obese subjects. Journal of Applied Physics, 2020, 128, .	2.5	4
110	Electrical conductivity imaging of lower extremities using MREIT: Postmortem swine and in vivo human experiments. , 2008, 2008, 5830-3.		3
111	Functional brain imaging using MREIT and EIT: Requirements and feasibility. , 2011, , .		3
112	Conductivity imaging of human lower extremity using MREIT with multi-echo pulse sequence and 3 mA imaging current. , 2011, , .		3
113	Multi-Channel Trans-Impedance Leadforming for Cardiopulmonary Monitoring: Algorithm Development and Feasibility Assessment Using <i>In Vivo</i> Animal Data. IEEE Transactions on Biomedical Engineering, 2022, 69, 1964-1974.	4.2	3
114	Conductivity Imaging of Postmortem and In-vivo Canine Brains using MREIT. , 2007, , .		2
115	High-resolution MREIT using low imaging currents. , 2011, 2011, 7025-8.		2
116	Analysis and Blocking of Error Propagation by Region-Dependent Noisy Data in MREIT. SIAM Journal of Scientific Computing, 2013, 35, B912-B924.	2.8	2
117	Tidal volume and stroke volume changes caused by respiratory events during sleep and their relationship with OSA severity: a pilot study. Sleep and Breathing, 2021, 25, 2025-2038.	1.7	2
118	Electrical Conductivity Imaging of Postmortem Canine Brains using Magnetic Resonance Electrical Impedance Tomography. Annual International Conference of the IEEE Engineering in Medicine and Biology Society, 2007, 2007, 4146-9.	0.5	1
119	Equivalent Isotropic Conductivity Image Reconstruction in MREIT. , 2007, , .		1
120	Experimental verification of contrast mechanism in Magnetic Resonance Electrical Impedance Tomography (MREIT). , 2010, 2010, 4987-90.		1
121	Three-dimensional MREIT simulator (MREITSim). , 2011, , .		1
122	Feasibility of dual-frequency conductivity imaging using MREIT and MREPT. , 2011, , .		1
123	In vivo MREIT conductivity imaging of canine brain to evaluate ischemia and abscess. , 2011, , .		1
124	Modelling of electromagnetic field distribution for optimising electrode configurations in liver MRâ€based electrical impedance tomography. Electronics Letters, 2014, 50, 1273-1275.	1.0	1
125	Conductivity image enhancement in MREIT using adaptively weighted spatial averaging filter. BioMedical Engineering OnLine, 2014, 13, 87.	2.7	1
126	Evaluation of three-dimensional anisotropic head model for mapping realistic electromagnetic fields of brain tissues. AIP Advances, 2015, 5, 087152.	1.3	1

#	Article	IF	CITATIONS
127	Principles and Use of Magnetic Resonance Electrical Impedance Tomography in Tissue Electroporation. , 2016, , 1-18.		1
128	Evaluation of electrical conductivity and anisotropy in muscle tissues using conductivity tensor imaging (CTI). AIP Advances, 2020, 10, 115115.	1.3	1
129	Respiration monitoring in PACU using ventilation and gas exchange parameters. Scientific Reports, 2021, 11, 24312.	3.3	1
130	Three-dimensional forward problem in magnetic resonance electrical impedance tomography (MREIT). , 0, , .		0
131	Magnetic resonance electrical impedance tomography (MREIT): phantom experiments for static resistivity images using J-substitution algorithm. , 0, , .		Ο
132	Recent Development of Magnetic Resonance Electrical Impedance Tomography toward High-Resolution Conductivity Imaging. , 2007, , .		0
133	Animal and human imaging experiments in magnetic resonance electrical impedance tomography (MREIT). , 2009, 2009, 3165-8.		Ο
134	Numerical simulation of frequency-difference EIT using multi-shell concentric spherical head model. , 2011, , .		0
135	Potential of MREIT conductivity imaging to detect breast cancer: Experimental and numerical simulation studies. , 2012, 2012, 440-3.		0
136	Enhanced magnetic flux density mapping using coherent steady state equilibrium signal in MREIT. AIP Advances, 2016, 6, 035121.	1.3	0
137	Principles and Use of Magnetic Resonance Electrical Impedance Tomography in Tissue Electroporation. , 2017, , 549-565.		0
138	ELECTRICAL IMPEDANCE TOMOGRAPHY FOR IMAGING AND LESION ESTIMATION. , 2005, , 193-239.		0